Science Advances

AAAS

advances.sciencemag.org/cgi/content/full/3/6/e1603203/DC1

Supplementary Materials for

A general strategy to synthesize chemically and topologically anisotropic Janus particles

Jun-Bing Fan, Yongyang Song, Hong Liu, Zhongyuan Lu, Feilong Zhang, Hongliang Liu, Jingxin Meng, Lin Gu, Shutao Wang, Lei Jiang

Published 21 June 2017, *Sci. Adv.* **3**, e1603203 (2017)
DOI: 10.1126/sciadv.1603203

The PDF file includes:

- fig. S18. SEM images of the Janus particles capture and recognize spherical PS particles and live bacteria.
- table S1. Dissipative particle dynamics simulation interaction parameters between different types of beads.

Other Supplementary Material for this manuscript includes the following:
(available at advances.sciencemag.org/cgi/content/full/3/6/e1603203/DC1)

- movie S1 (.mp4 format). Polymerization of 15 min.

1. Anchoring monomer mediated emulsion interfacial polymerization systems for the synthesis of Janus particles

The effectiveness of anchoring monomer mediated interfacial polymerization: To demonstrate the effectiveness of interfacial polymerization, we firstly compared two polymerization systems into one of which hydrophilic anchoring monomers were introduced and the other was not preformed. After polymerization, crescent-moon shaped Janus particles were fabricated in the presence of hydrophilic AA while only spherical particles were formed in the absence of AA.

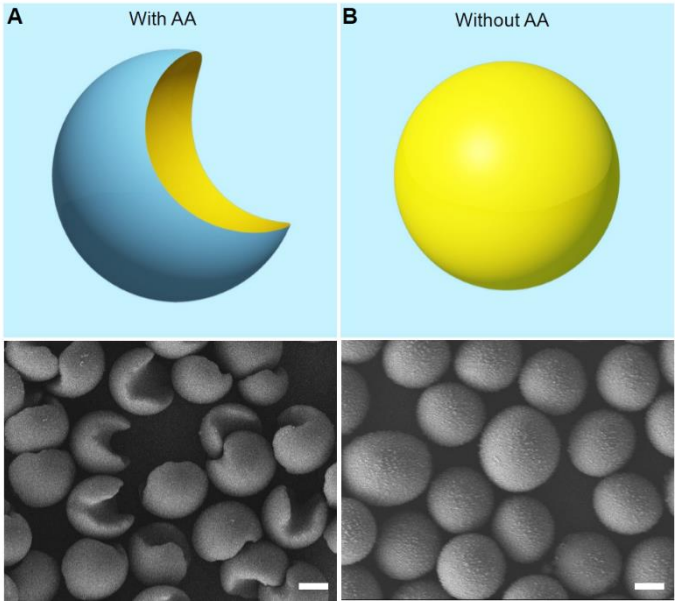

fig. S1. Anchoring monomer–mediated interfacial polymerization. (**A**) Crescent-moon shaped Janus particles are fabricated in the presence of anchoring monomer. (**B**) If without AA, only spherical particles are formed. Scale bar, 1 μm.

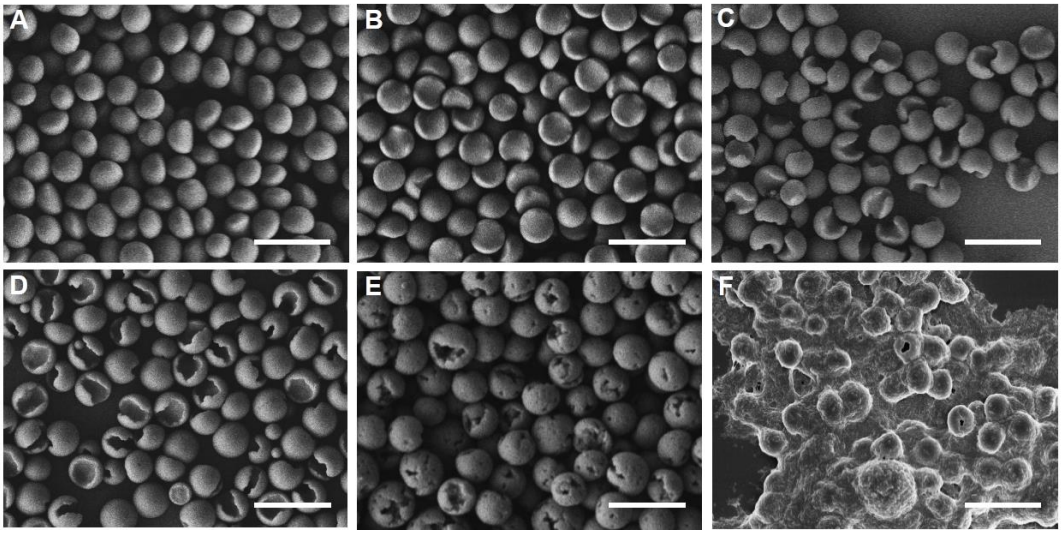

fig. S2. SEM image of topological particles and composite film. (**A**) Bread shaped Janus particles. (**B**) Hemispherical shaped Janus particles. (**C**) Crescent-moon shaped Janus particles. (**D**) Pistachio shaped Janus particles. (**E**) Porous particles. (**F**) Composite film. Scale bar, 5 μm.

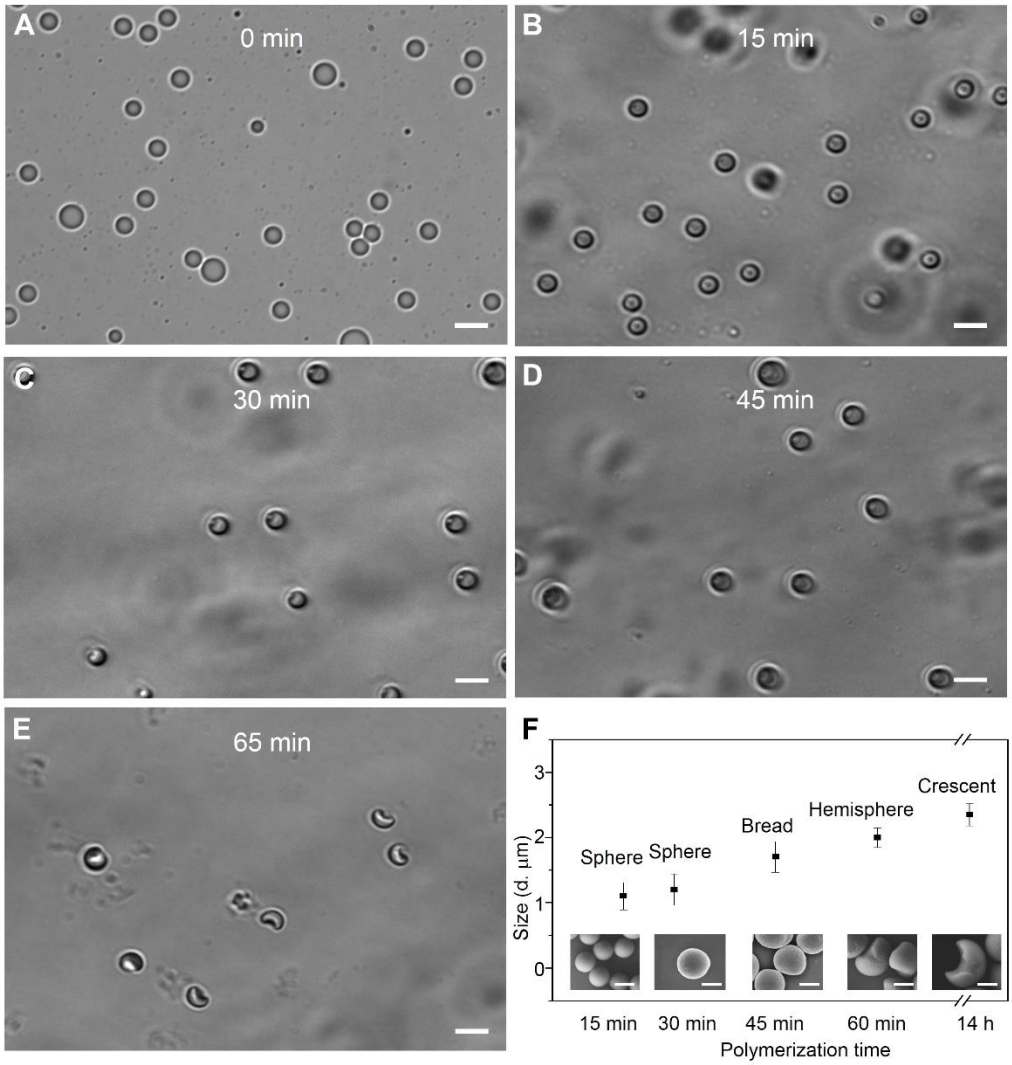

fig. S3. Time-dependent morphology and size evolution of typical crescent moon–shaped PSDVB ⊃ PAA particles. (**A** to **E**) Bright-field microscope images of time-dependent growth process of Janus particles. Scale bar, 5 μm. (**F**) with the increase of the polymerization time, the size of particles increased and their topology gradually changed from sphere, bread, hemisphere to crescent-moon. Scale bar, 1 μm.

2. The mechanism of preferential growth of particle at the edge of interface

For the system comprising two immiscible monomers phase at equilibrium, the chemical potential $\Delta\overline{G}_{m,o}$ of hydrophobic monomer in the oil phase should be equal to the chemical potential $\Delta\overline{G}_{m,a}$ of hydrophilic monomer in the aqueous phase. The particle grows up because of the increased chemical potential. When a new

equilibrium appears, the difference of chemical potential again equals to zero (*23*). Therefore, under every equilibrium stage of polymerization

$$\Delta\overline{G}_{m,o} - \Delta\overline{G}_{m,a} = 0 \qquad (1)$$

The chemical potential $\Delta\overline{G}_{m,a}$ of hydrophilic monomer in the aqueous phase, can be expressed as following (*23, 24*)

$$\Delta\overline{G}_{m,a} = RT[\ln\phi_{ma} + (1-m^*_{ma})(1-\phi_{ma}) + \chi_{ma}(1-\phi_{ma})^2] \qquad (2)$$

where R is the gas constant, T is the absolute temperature, ϕ_{ma} is the volume fraction of monomer in the aqueous phase, m^*_{ma} is the segment volume ratio, and χ_{ma} is the monomer-water interaction parameter.

The chemical potential $\Delta\overline{G}_{m,o}$ of hydrophobic monomer in the oil phase are usually approximated as the sum of the three contributions: i) $\Delta\overline{G}_m$, the monomer-polymer mixing forces, ii) $\Delta\overline{G}_{el}$, the polymer network elastic-retractive force, and iii) $\Delta\overline{G}_t$, the particle-water interfacial tension force. Therefore, according to the Flory-Huggins expression for $\Delta\overline{G}_m$ (*25*), the Flory-Rehner equation for $\Delta\overline{G}_{el}$ (*25*), and the Morton equation for $\Delta\overline{G}_t$ (*26*), the $\Delta\overline{G}_{m,o}$ can be expressed as following

$$\Delta\overline{G}_{m,o} = RT[\ln(1-\nu_p) + (1-\frac{1}{j})\nu_p + \chi_{mp}\nu_p^{\,2}] + R\,T\,N_m V_m(\nu_p^{\frac{1}{3}} - \frac{\nu_p}{2}) + \frac{2V_m\gamma}{r} \qquad (3)$$

where ν_p is volume fraction of polymer in the oil phase, *j* is the number average degree of polymerization of the polymer, χ_{mp} is the monomer-polymer interaction parameter, *N* is the effective number of chains in the network per unit volume, and V_m is the molar volume of the monomer, γ is the particle-water interfacial tension, and r is the radius of the droplet.

As the temperature is raised from 40 ^{o}C to 70 ^{o}C, the polymerization can be triggered. The free radicals from water insoluble 2, 2′-azobisisobutyronitrile (AIBN) are initially generated inside droplets (oil phase) and subsequently initiate the polymerization of

hydrophobic St and DVB, resulting in the formation of a crosslinked particle nucleus within droplet. Therefore, from equation (3), the chemical potential $\Delta\overline{G}_{m,o}$ of hydrophobic phase increases preferentially at the initial polymerization. However, when the particle nucleus moves to the interface and initiates the polymerization of hydrophilic AA, the chemical potential $\Delta\overline{G}_{m,a}$ is increased to counteract the increase of $\Delta\overline{G}_{m,o}$. Therefore, to maintain the chemical potential equilibrium, the subsequent polymerization would be confined at the interface of droplets, where the hydrophilic monomer and hydrophobic monomer would continually diffuse toward the interface and preferentially copolymerize.

3. Computer simulation of the growth of Janus particle

We employ dissipative particle dynamics simulations coupled with the stochastic reaction model (*27*, *28*) to describe the generic growth process of particle at the interface.

3.1 Model construction

In our simulations, the model is constructed by generating a spherical hydrophobic droplet in the water phase. The box is constructed with a size of 35^3 of reduced units (see below). The hydrophobic droplet is a spherical region with the radius of R=10.5 in the middle of the box. The styrene (S) beads and DVB (V) beads (DVB molecule is coarse-grained as N=2 oligomer) are randomly distributed in the hydrophobic droplet with the total particle number density ρ=3.0 to form the bulk hydrophobic phase. A piece of network structure with the bead type (P) is put at the interface of the two phases with a small radius of r=3 to represent the crosslinked particle nucleus that moves to the oil/water interface to induce the copolymerization at the interface (the network structure is made by connecting the middle monomers of linear PS chains with N=3). The rest space of the simulation box (outside of the spherical hydrophobic droplet) is filled with solvent (W) and the AA monomer (A) with the concentration of $[AA_0]$. The initial configuration is schematically shown in fig. S4.

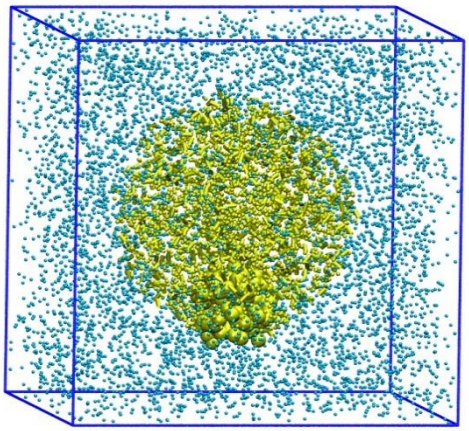

fig. S4. Schematic illustration of the initial configuration of the simulations. The spherical droplet in the middle of simulation box shows the hydrophobic phase filled with styrene (S, yellow) and DVB (V, yellow) beads. The small deep yellow ball at the interface is the particle nucleus P (deep yellow). The rest of the box is filled with solvent (not shown for clarity) and the hydrophilic AA (A, blue) beads.

3.2 The dissipative particle dynamics simulation method

In dissipative dynamics simulations, the time evolution of interacting beads is governed by Newton's equations of motion (*29*). Inter-bead interactions are characterized by pair wise conservative (F^C), dissipative (F^D), and random forces (F^R) acting on bead *i* by bead *j*. They are given by

$$\mathbf{F}_{ij}^{C} = -\alpha_{ij}\omega^{C}(r_{ij})\mathbf{e}_{ij} \tag{1}$$

$$\mathbf{F}_{ij}^{D} = -\gamma\omega^{D}(r_{ij})(\mathbf{v}_{ij}\cdot\mathbf{e}_{ij})\mathbf{e}_{ij} \tag{2}$$

$$\mathbf{F}_{ij}^{R} = \sigma\omega^{R}(r_{ij})\xi_{ij}\Delta t^{-1/2}\mathbf{e}_{ij} \tag{3}$$

where $\mathbf{r}_{ij} = \mathbf{r}_i - \mathbf{r}_j$, $r_{ij} = |\mathbf{r}_{ij}|$, $\mathbf{e}_{ij} = \mathbf{r}_{ij}/r_{ij}$, and $\mathbf{v}_{ij} = \mathbf{v}_i - \mathbf{v}_j$. ξ_{ij} is a random number with zero mean and unit variance. For easy numerical handling, the cutoff radius, the bead mass, and the temperature are often set to be the units, i.e., $r_c = m = k_B T = 1$. α_{ij} is the repulsion strength which describes the maximum repulsion between interacting beads. ω^C, ω^D, and ω^R are three weight functions for the conservative, dissipative and random forces, respectively. For the conservative force, $\omega^C(r_{ij}) = 1 - r_{ij}/r_c$ $(r_{ij} < r_c)$ and $\omega^C(r_{ij}) = 0$ $(r_{ij} \geq r_c)$. $\omega^D(r_{ij})$ and $\omega^R(r_{ij})$ have a relation according to the

fluctuation–dissipation theorem (*30*)

$$\omega^D(r_{ij}) = [\omega^R(r_{ij})]^2 \tag{4}$$

$$\sigma^2 = 2\gamma k_B T \tag{5}$$

Here we choose a simple form of ω^D and ω^R due to Groot and Warren (*31*)

$$\omega^D(r_{ij}) = [\omega^R(r_{ij})]^2 = \begin{cases} (1 - r_{ij}/r_c)^2 & (r < r_c) \\ 0 & (r \geq r_c) \end{cases} \tag{6}$$

Groot–Warren-velocity Verlet algorithm (*29, 31*) is used here to integrate the Newton's equations of motion,

$$\mathbf{r}_i(t + \Delta t) = \mathbf{r}_i(t) + \Delta t \mathbf{v}_\mathbf{i}(t) + 1/2(\Delta t)^2 \mathbf{f}_i(t)$$

$$\tilde{\mathbf{v}}_i(t + \Delta t) = \mathbf{v}_i(t) + \lambda \Delta t \mathbf{f}_i(t)$$

$$\mathbf{f}_i(t + \Delta t) = \mathbf{f}_i[\mathbf{r}(t + \Delta t), \tilde{\mathbf{v}}(t + \Delta t)]$$

$$\mathbf{v}_i(t + \Delta t) = \mathbf{v}_i(t) + 1/2 \Delta t(\mathbf{f}_i(t) + \mathbf{f}_i(t + \Delta t)) \tag{7}$$

Here, $\lambda = 0.65$ according to Ref. 31. In dissipative particle dynamics simulations, polymers are constructed by connecting the neighboring beads together via the harmonic springs $\mathbf{F}_i^S = \sum_j C\mathbf{r}_{ij}$. We choose the spring constant $C = 10$ according to Ref. 31. In this study, we choose the time step $\Delta t = 0.05$ in the dissipative particle dynamics simulations. The dissipative dynamics simulation interactions between different types of beads are shown in table S1.

table S1. Dissipative particle dynamics simulation interaction parameters between different types of beads.

Bead type	*S*	*A*	*P*	*W*	*V*
S	25.0	45.0	27.0	45.0	25.0
A		25.0	30.0	25.0	45.0
P			25.0	45.0	35.0
W				25.0	65.0
V					25.0

3.3 Stochastic Reaction Model

The copolymerization reactions are described by the generic stochastic reaction model proposed in previous works (*27*, *28*).

In this reaction model, we introduce the idea of reaction probability P_r to control the reaction process. In each reaction time interval τ, if an active center meets several polymerizable monomers in the reaction radius, firstly it randomly chooses one of the monomer as a reacting candidate. Subsequently, another random number P is generated. And then, by checking if it is smaller than the preset reaction probability P_r, we decide whether the chosen polymerizable monomer will connect with the active end or not. This process in one reaction step is schematically illustrated in fig. S5. If the bond can be formed between the active end and the reacting monomer, we record the connection information and update the spring forces between them.

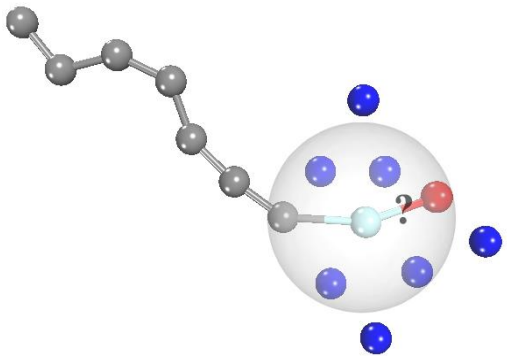

fig. S5. Illustration of the reaction process controlled by the reaction probability and reaction radius in the copolymerization. When the active center (the cyan ball) meets several free monomers (some of the blue balls, including the red ball) in its reaction radius (the semitransparent sphere), it randomly chooses one of the monomers as a reacting object (the red ball). Then the generation of the bond between the cyan ball and the red ball is determined by the preset reaction probability.

This idea of reaction is especially suitable for the design of polymerization-type reactions. During the polymerization, the newly connected monomers then turn to be the living centers in the next propagation step of the same chain to connect other free monomers, so that the active end is transferred forward.

Assuming that we are now simulating a living polymerization-type reaction, there are basically three types of reactions included

$$\begin{aligned} &I^{*}+M \rightarrow I-P^{*} \\ &I-P^{*}+M \rightarrow I-P-P^{*} \\ &I-P_{n-1}-P^{*}+M \rightarrow I-P_{n}-P^{*} \quad (n=2,3,4..) \end{aligned} \tag{8}$$

in which "I^{*}" and "I" denote the active and the dead initiator, respectively. "P^{*}" and "P" are the active chain end and the reacted chain monomer, respectively, and "M" is the free monomer. If we focus on the living polymerization, i.e., there is no chain termination reaction, the reaction rate r_p can be expressed as

$$r_p = -k[P^{*}][M] \tag{9}$$

where [P^{*}] and [M] are the concentrations of active chain ends and free monomers, respectively, and k is the reaction rate coefficient.

Based on predefined reaction probability P_r and uniformly generated random number, it is easy to conclude that the average consumed number of free monomers in one propagation step is $N_{P*}P_r$, where N_{P*} is the number of active ends in the system. Since we are considering the living polymerization, any radical termination and bi-radical termination are neglected, thus the value of N_{P*} is always equivalent to the number of free radicals at the beginning. Therefore, we obtain the average consumed number of free monomers in one time unit as $N_{P*}P_r\tau$. Consequently, the concentration change of the free monomers in one time unit is given by

$$d[M] = \frac{N_{P*} \cdot P_r \cdot \tau}{V \cdot Na} = \frac{[P*] \cdot P_r \cdot \tau}{Na} \tag{10}$$

where $[M]$ is the concentration of free monomers, V is the volume of the system and Na is the Avogadro's number. As a result, we can obtain the reaction rate as

$$r_p = -\frac{d[M]}{dt} = \frac{[P*] \cdot P_r \cdot \tau}{Na \cdot t_0} \tag{11}$$

where t_0 is the real time unit in the simulation. Based on this equation, in this study we assume that different reaction probabilities correspond to different reaction rates of the systems determined by different levels of reaction activation energies. This generic stochastic reaction model had been successfully used to describe the polymerizations in different conditions, such as polymerization induced phase separation (*27*) and surface-initiated polymerization on the flat substrate (*28*), on the concave surface (*32*), and on the convex NP surface (*33*). This generic reaction model had also been used to describe other types of reactions, e.g., curing reactions in epoxy resin systems (*34*). In practice we define the reaction probability as $P_r^0 = 0.005$ (between bead types S, A, P, V) to represent the generic copolymerization with the same time interval $\tau = 20\Delta t = 1.0$ of reduced time unit.

3.4 Simulation details

The goal of our simulation is to clarify the mechanism of the anisotropic growth of

particle. Therefore, a series of dissipative particle dynamics simulations are carried out in constant-volume and constant-temperature (NVT) conditions. All the simulations are carried out using GPU accelerated large-scale molecular simulation toolkit (GALAMOST) (*35*). As illustrated in fig. S4, the periodic boundary conditions are applied in X, Y, and Z directions in our simulations. 133 short chains (N=3) are put together to form a living center with size of r=3. One of the two PS chain ends is the active center, which will be the starting point of the copolymerization. The individual styrene and AA beads are set as free monomers for the copolymerization. The two beads in N=2 DVB molecule are both reactive, so that the network structure during the copolymerization can be obtained, in which the DVB molecules will be the crosslinking points. The monomer concentration of AA in the hydrophilic phase is set as $[AA_0]$ = 0.33 monomers/σ^3, where σ is the reduced unit of the length scale. A period of 4×10^4 time steps simulation is first conducted to relax the configuration. Following up is the 2×10^5 (for P_r^0 and $5P_r^0$) or 6×10^5 (for $P_r^0/5$) time steps dissipative particle dynamics simulation production run. We analyze the morphology evolution during the polymerization and especially focus on the final particle structure after the polymerization.

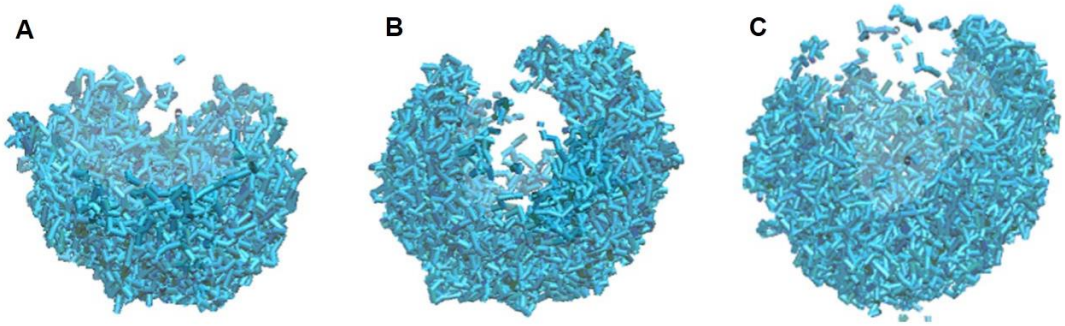

fig. S6. The influence of the concentration of AA on the morphology of Janus particle. (**A**) 0.75$[AA_0]$. (**B**) $[AA_0]$. (**C**) 1.25$[AA_0]$.

To clarify the influence of concentration of the hydrophilic monomer on the morphology of particle, we design simulation systems with the same styrene and DVB concentrations and the same copolymerization rate (with the reaction probability Pr^0 and reaction time interval τ) but with different concentrations of hydrophilic AA

monomers (as compared to the reference concentration [AA_0]). To clearly observe the structure, the inner layer composed of hydrophobic polymer is not shown. With the increase of AA concentration, the hemisphere, crescent-moon and pistachio shaped Janus particle can be observed, which is in agreement with the experimental results. We further study the influence of hydrophobic monomers on the morphologies of particle. As shown in fig. S7, with the increase of the amount of hydrophobic monomers in the hydrophobic phase (with the reference of the number of monomers *N*), we can observe the variations of the particle morphologies from hemisphere to crescent-moon and then to sphere structures.

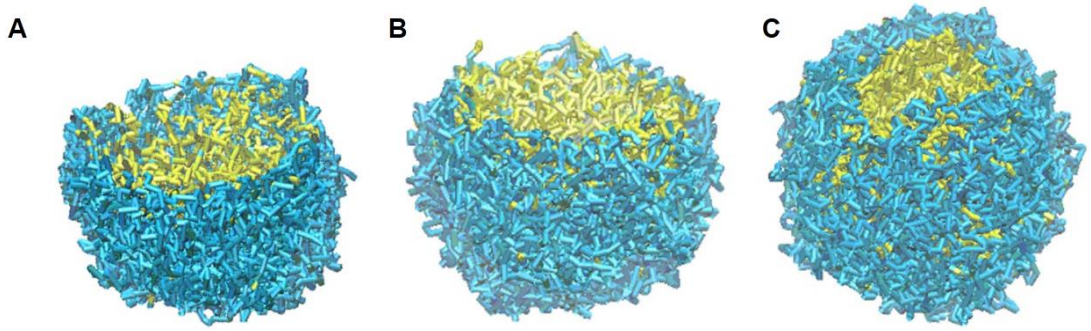

fig. S7. The influence of the number of hydrophobic monomer beads on the morphology of particle. (**A**) 0.5*N*. (**B**) *N*. (**C**) 1.25*N*. The number of hydrophobic monomers is adopted to represent the influence of concentration of hydrophobic monomers. With the increase of the number of hydrophobic monomers, the hemispherical particle, crescent-moon shaped particle and spherical particle can be observed.

4. Detailed experimental conditions for the synthesis of a large variety of Janus particles with crescent-moon shaped topology

PS spheres synthesis. The noncrosslinked PS spheres were synthesized by one-step soap-free polymerization method. The different size of PS particles were synthesized by varying the molar quantities of styrene. In a typical synthesis, 56 mmol styrene, 1.7 mmol sodium chloride and 0.3 mmol ammonium persulfate (APS) were dispersed in 60 mL deionized water. After deoxygenation bubbled with N_2 for 30 min at room temperature, the solution was polymerized at 70 ^oC for 24 h. Then, the resultant particles were washed with ethanol and deionized water for three times. Finally, the

PS particles were re-dispersed in deionized water and freeze-dried.

Fluorescent PS spheres synthesis. Firstly, 0.25 mmol 9-vinylanthracene was dissolved in 56 mmol styrene. Then the styrene solution was added into 60 mL aqueous solutions containing 1.7 mmol sodium chloride and 0.3 mmol APS. After deoxygenation bubbled with N_2 for 30 min at room temperature, the solution was polymerized at 70 ^oC for 24 h. Then, the resultant particles were washed with ethanol and deionized water for three times. Finally, the fluorescent PS particles were re-dispersed in deionized water and freeze-dried.

The generality for the fabrication of a large variety of Janus particles. A series of hydrophilic monomers were employed to demonstrate the effectiveness of this method in yielding high quality anisotropic Janus particles. The detailed fabrication process is shown as follow. The size of PS spheres used here is 1.08 ± 0.05 μm.

1. **PSDVB ⊃ PHEA Janus particles synthesis.** 10 mL of 1% v/v 1-chlorodecane (CD) oil-in-water emulsion containing 0.25% w/v sodium dodecyl sulfate (SDS) was mixed with 20 mL of aqueous solution (containing 0.25% w/v SDS) of 1% w/v polystyrene particles at 40 ^oC. After 16 h, 10 mL oil-in-water emulsion (containing 0.25% w/v SDS), composed of 13 mmol St, 7 mmol DVB, 0.24 mmol AIBN and 2.6 mmol hydrophilic anchoring monomer hydroxyethyl acrylate (HEA), was prepared by ultrasonic emulsification and subsequently was added into above solution at 40 ^oC for 6 h. After additional adding 5 mL of 1% w/v PVA into the mixture and then deoxygenation bubbled with N_2 for 15 min at room temperature, the polymerization was performed at 70 ^oC for 14 h.

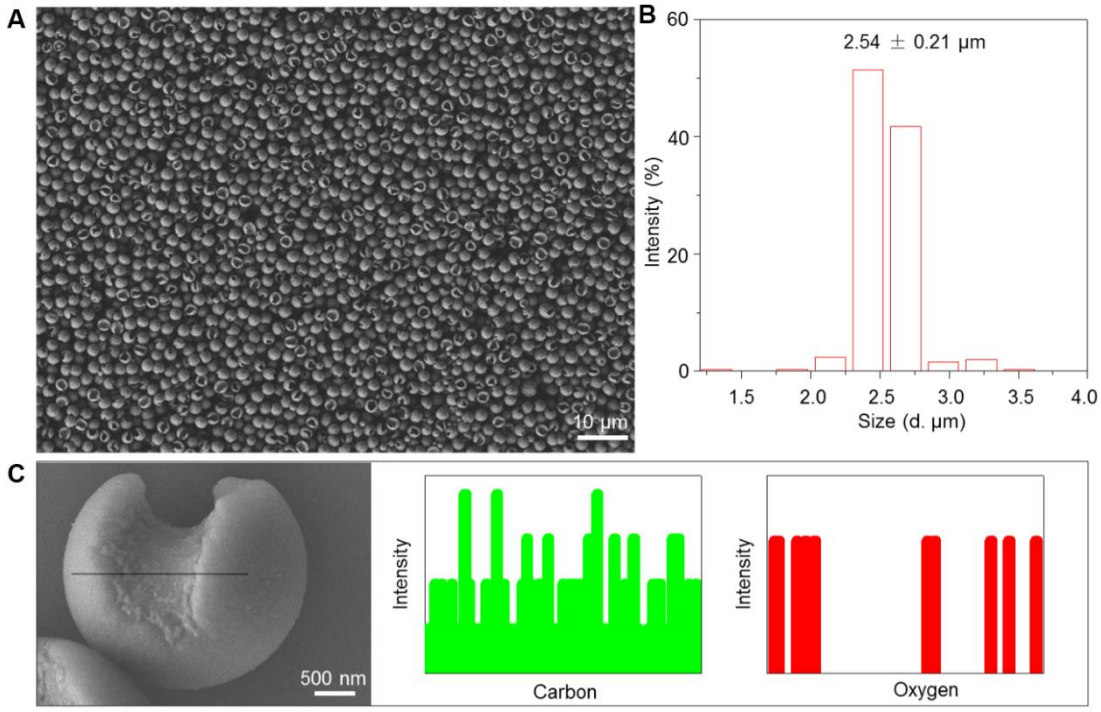

fig. S8. Characterization of crescent moon–shaped PSDVB ⊃ PHEA particles. (**A**) SEM image of large area of particles. (**B**) Particle size distributions analysis of particles. 300 particles are measured to get the size distributions. (**C**) Energy dispersive X-ray spectroscopy (EDX) analysis of particles. The convex region of particles is PHEA and therefore the detected elements include C and O, while the concave region is poly(styrene-co-divinyl benzene) and the detected element is C. The results reveal distinct element distributions on the convex surface and concave surface of Janus particles.

2. **PSDVB ⊃ PMAH Janus particles synthesis.** 10 mL of 1% v/v CD oil-in-water emulsion containing 0.25% w/v SDS was mixed with 20 mL of aqueous solution (containing 0.25% w/v SDS) of 1% w/v polystyrene particles at 40 ^{o}C. After 16 h, 10 mL oil-in-water emulsion (containing 0.25% w/v SDS), composed of 13 mmol St, 7 mmol DVB, 0.24 mmol AIBN and 7 mmol hydrophilic anchoring monomer maleic anhydride (MAH), was prepared by ultrasonic emulsification and subsequently was added into above solution at 40 ^{o}C for 6 h. After additional adding 5 mL of 1% w/v PVA into the mixture and then deoxygenation bubbled with N_2 for 15 min at room temperature, the polymerization was performed at 70 ^{o}C for 14 h.

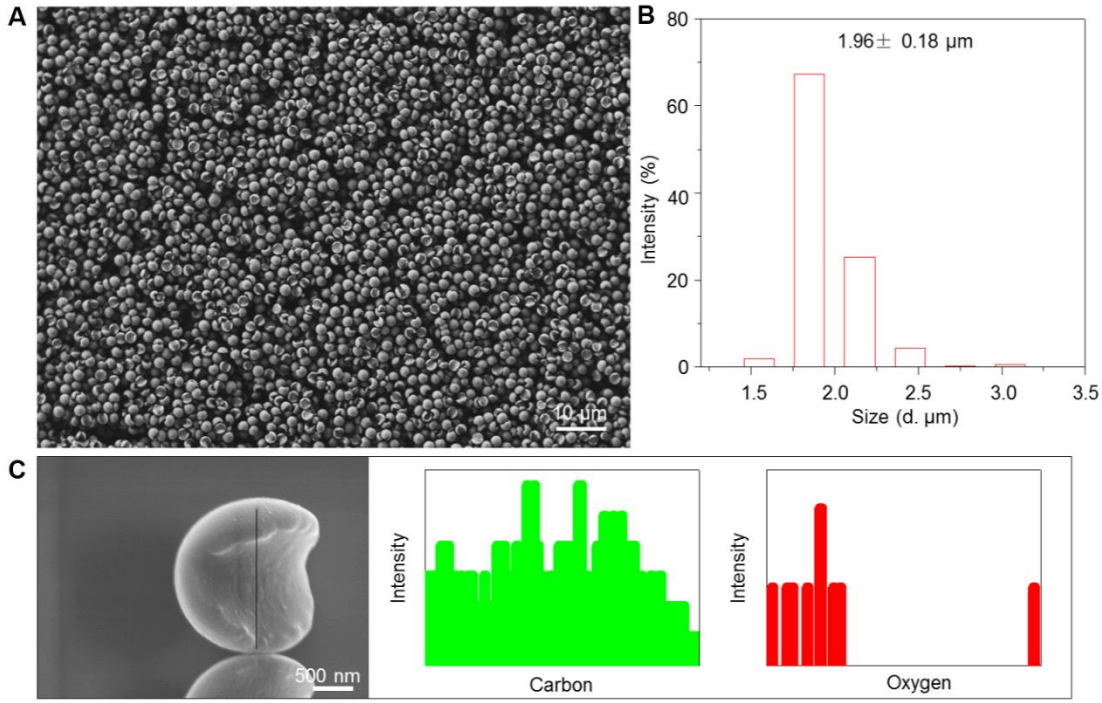

fig. S9. Characterization of crescent moon–shaped PSDVB ⊃ PMAH Janus particles. (**A**) SEM image of large area of particles. (**B**) Particle size distribution analysis of the crescent-moon shaped particles. 300 particles are measured to get the size distribution. (**C**) EDX analysis of particles. The convex region of particles is PMAH and therefore the detected elements include C and O, while the concave region is poly(styrene-co-divinyl benzene) and the detected elements is C. The results reveal distinct element distributions on the convex surface and concave surface of Janus particles.

3. **PSDVB ⊃ PHEMA Janus particles synthesis.** 10 mL of 1% v/v CD oil-in-water emulsion containing 0.25% w/v SDS was mixed with 20 mL of aqueous solution (containing 0.25% w/v SDS) of 1% w/v polystyrene particles at 40 ^{o}C. After 16 h, 10 mL oil-in-water emulsion (containing 0.25% w/v SDS), composed of 13 mmol St, 7 mmol DVB, 0.24 mmol AIBN and 7 mmol hydrophilic anchoring monomer hydroxyethyl methacrylate (HEMA) with 50 μL acetic acid, was prepared by ultrasonic emulsification and subsequently was added into above solution at 40 ^{o}C for 6 h. After additional adding 5 mL of 1% w/v PVA into the mixture and then deoxygenation bubbled with N_2 for 15 min at room temperature, the polymerization was performed at 70 ^{o}C for 14 h.

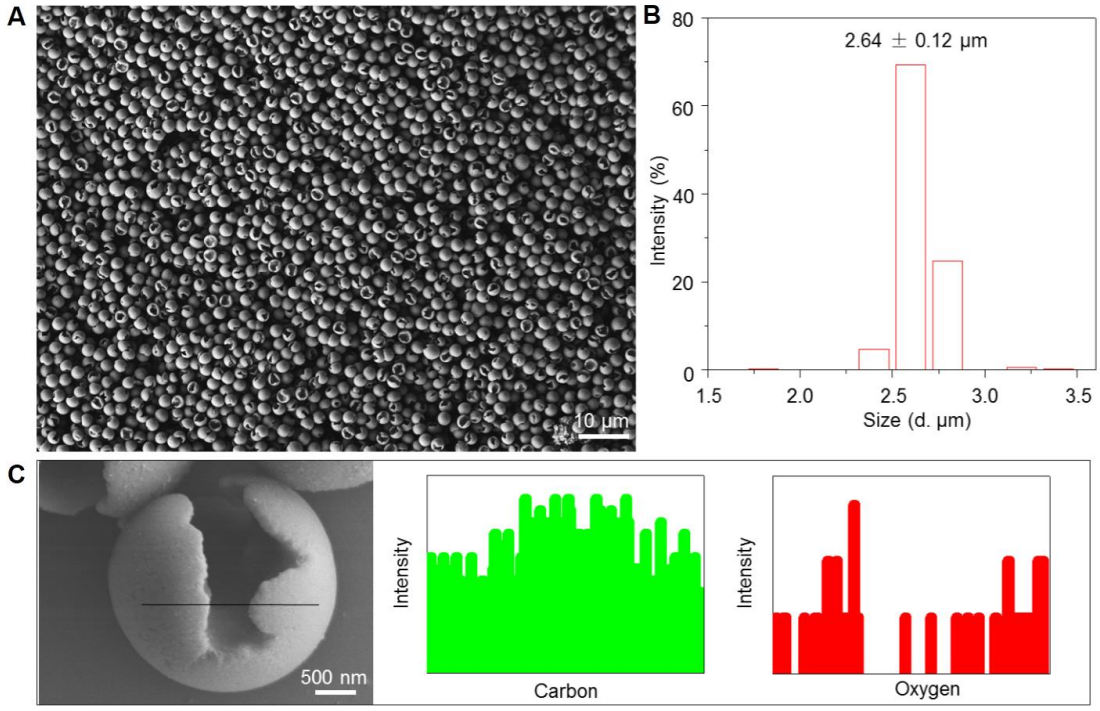

fig. S10. Characterization of crescent moon–shaped PSDVB ⊃ PHEMA particles. (**A**) SEM image of large area of particles. (**B**) Particle size distribution analysis of the crescent-moon shaped particles. 300 particles are measured to get the size distribution. (**C**) EDX analysis of particles. The convex region of particles is PHEMA and therefore the detected elements include C and O, while the concave region is poly(styrene-co-divinyl benzene) and the detected elements is C. The results reveal distinct element distributions on the convex surface and concave surface of Janus particles.

4. **PSDVB ⊃ PMA Janus particles synthesis.** 10 mL of 1% v/v CD oil-in-water emulsion containing 0.25% w/v SDS was mixed with 20 mL of aqueous solution (containing 0.25% w/v SDS) of 1% w/v polystyrene particles at 40 ^{o}C. After 16 h, 10 mL oil-in-water emulsion (containing 0.25% w/v SDS), composed of 13 mmol St, 7 mmol DVB, 0.24 mmol AIBN and 7 mmol hydrophilic anchoring monomer maleic acid (MA), was prepared by ultrasonic emulsification and subsequently was added into above solution at 40 ^{o}C for 6 h. After additional adding 5 mL of 1% w/v PVA into the mixture and then deoxygenation bubbled with N_2 for 15 min at room temperature, the polymerization was performed at 70 ^{o}C for 14 h.

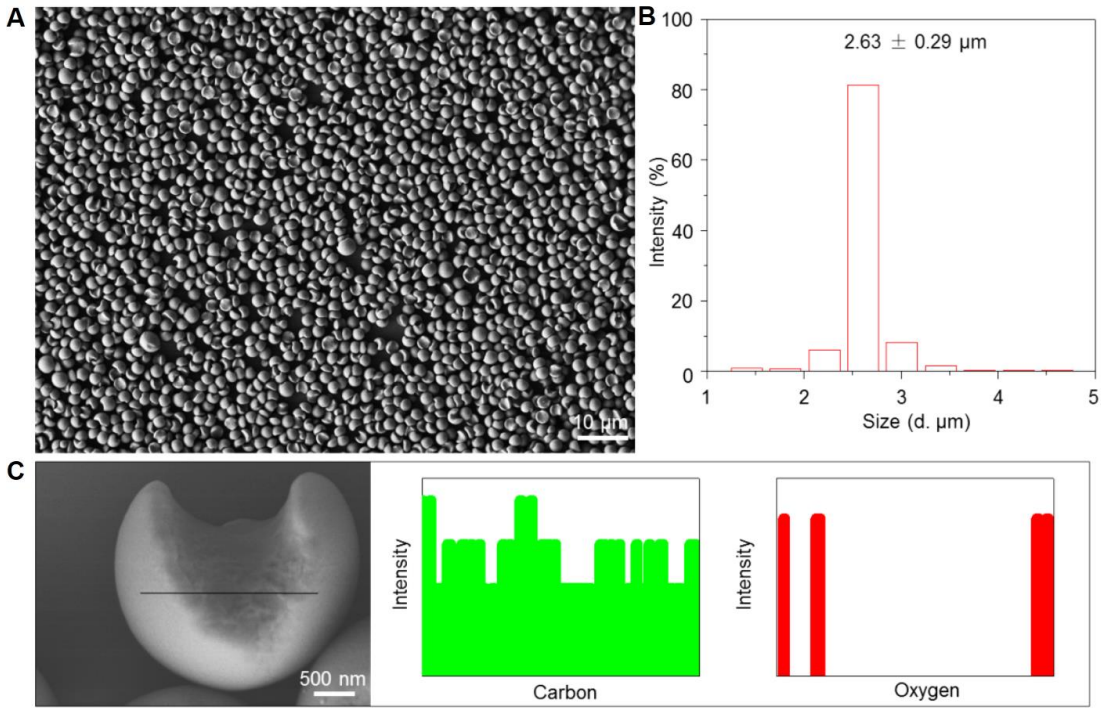

fig. S11. Characterization of crescent moon–shaped PSDVB ⊃ PMA Janus particles. (**A**) SEM image of large area of particles. (**B**) Particle size distribution analysis of the crescent-moon shaped particles. 300 particles are measured to get the size distribution. (**C**) EDX analysis of Janus particles. The convex region of particles is PMA and therefore the detected elements include C and O, while the concave region is poly(styrene-co-divinyl benzene) and the detected elements is C. The results reveal distinct element distributions on the convex surface and concave surface of particles.

5. **PSDVB ⊃ PIA Janus particles synthesis.** 10 mL of 1% v/v CD oil-in-water emulsion containing 0.25% w/v SDS was mixed with 20 mL of aqueous solution (containing 0.25% w/v SDS) of 1% w/v polystyrene particles at 40 ^{o}C. After 16 h, 10 mL oil-in-water emulsion (containing 0.25% w/v SDS), composed of 13 mmol St, 7 mmol DVB, 0.24 mmol 2, 2'-Azoisobutyronitrile (AIBN) and 7 mmol hydrophilic anchoring monomer itaconic acid (IA), was prepared by ultrasonic emulsification and subsequently was added into above solution at 40 ^{o}C for 6 h. After additional adding 5 mL of 1% w/v PVA into the mixture and then deoxygenation bubbled with N_2 for 15 min at room temperature, the polymerization was performed at 70 ^{o}C for 14 h.

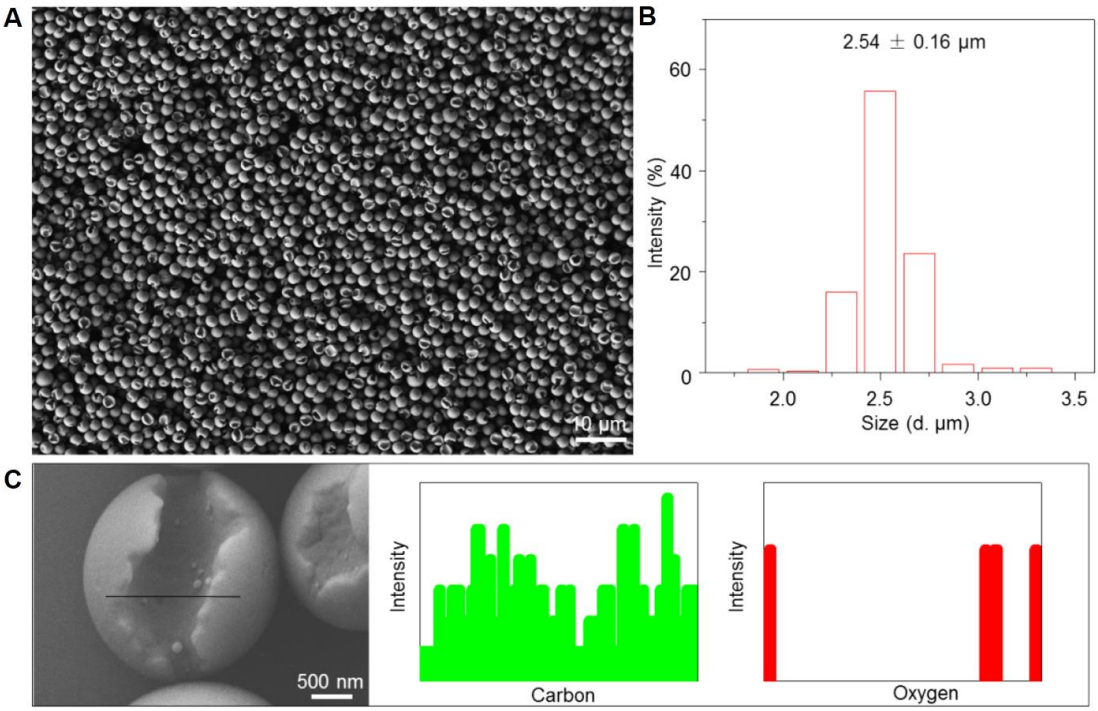

fig. S12. Characterization of crescent moon–shaped PSDVB ⊃ PIA particles. (**A**) SEM image of large area of particles. (**B**) Particle size distribution analysis of the crescent-moon shaped particles. 300 particles are measured to get the size distribution. (**C**) EDX analysis of Janus particles. The convex region of particles is PIA and therefore the detected elements include C and O, while the concave region is poly(styrene-co-divinyl benzene) and the detected elements is C. The results reveal distinct element distributions on the convex surface and concave surface of particles.

6. **PSDVB ⊃ PAM Janus particles synthesis.** 10 mL of 1% v/v CD oil-in-water emulsion containing 0.25% w/v SDS was mixed with 20 mL of aqueous solution (containing 0.25% w/v SDS) of 1% w/v polystyrene particles at 40 ºC. After 16 h, 10 mL oil-in-water emulsion (containing 0.25% w/v SDS), composed of 13 mmol St, 7 mmol DVB, 0.24 mmol 2, 2'-Azoisobutyronitrile (AIBN) and 7 mmol hydrophilic anchoring monomer acrylamide (AM), was prepared by ultrasonic emulsification and subsequently was added into above solution at 40 ºC for 6 h. After additional adding 5 mL of 1% w/v PVA into the mixture and then deoxygenation bubbled with N_2 for 15 min at room temperature, the polymerization was performed at 70 ºC for 14 h.

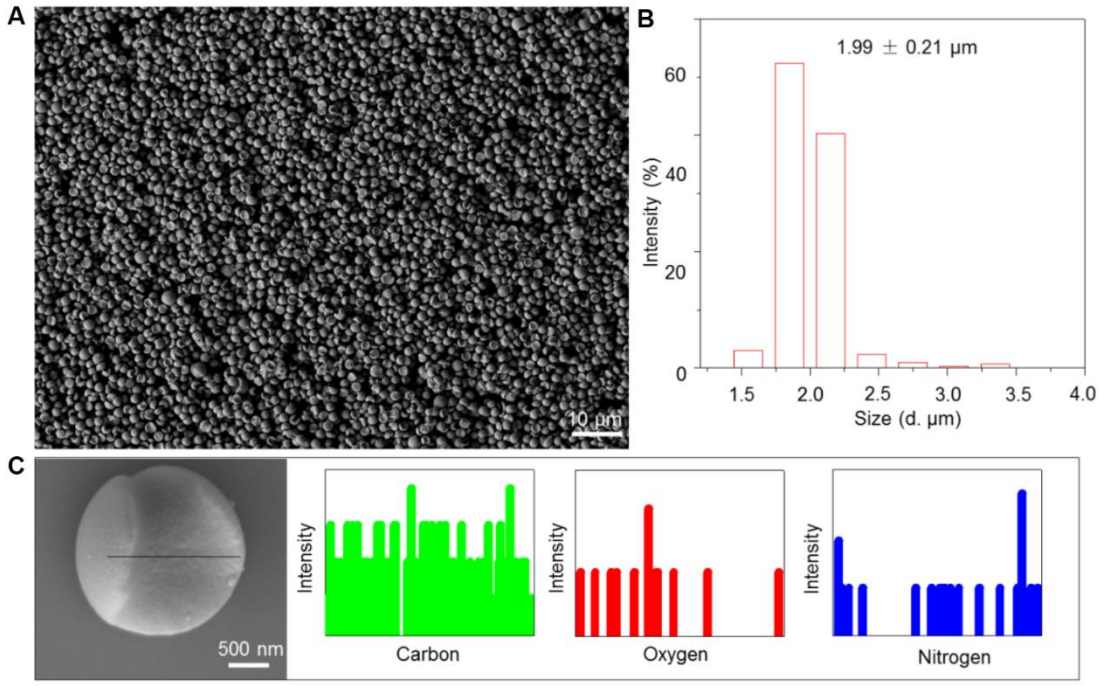

fig. S13. Characterization of crescent moon–shaped PSDVB ⊃ PAM particles. (**A**) SEM image of large area of particles. (**B**) Particle size distribution analysis of the crescent-moon shaped particles. 300 particles are measured to get the size distribution. (**C**) EDX analysis of Janus particles. The convex region of particles is PAM and therefore the detected elements include C, O and N, while the concave region is poly(styrene-co-divinyl benzene) and the detected elements only is C. The results reveal distinct element distributions on the convex surface and concave surface of particles.

7. **PSDVB ⊃ PNIPAM Janus particles.** 10 mL of 1% v/v CD oil-in-water emulsion containing 0.25% w/v SDS was mixed with 20 mL of aqueous solution (containing 0.25% w/v SDS) of 1% w/v polystyrene particles at 40 ^{o}C. After 16 h, 10 mL oil-in-water emulsion (containing 0.25% w/v SDS), composed of 13 mmol St, 7 mmol DVB, 0.24 mmol 2, 2’-Azoisobutyronitrile (AIBN) and 7 mmol hydrophilic anchoring monomer N-Isopropyl acrylamide (NIPAM) with 9 μL hydrochloric acid, was prepared by ultrasonic emulsification and subsequently was added into above solution at 40 ^{o}C for 6 h. After additional adding 5 mL of 1% w/v PVA into the mixture and then deoxygenation bubbled with N_2 for 15 min at room temperature, the polymerization was performed at 70 ^{o}C for 14 h.

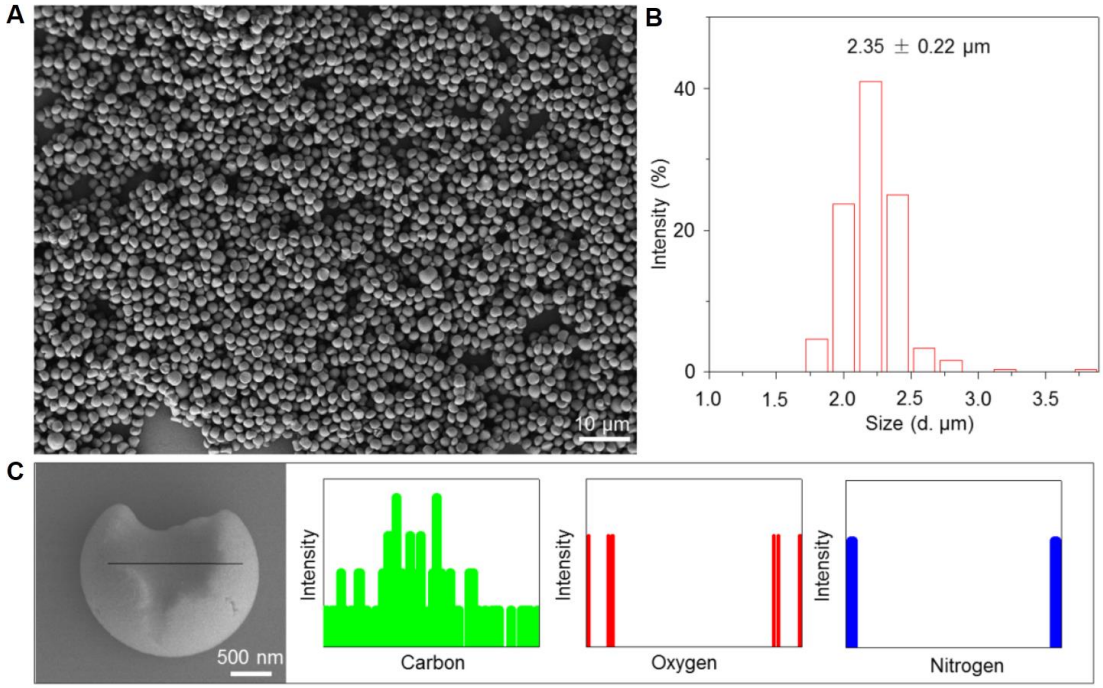

fig. S14. Characterization of crescent moon–shaped PSDVB ⊃ PNIPAM particles. (**A**) SEM image of large area of particles. (**B**) Particle size distribution analysis of particles. 300 particles are measured to get the size distribution. (**C**) EDX analysis of Janus particles. The convex region of particles is PNIPAM and therefore the detected elements include C, O and N, while the concave region is poly (styrene-co-divinyl benzene) and the detected elements only is C. The results reveal distinct element distributions on the convex surface and concave surface of particles.

8. **PSDVB ⊃ PMAM Janus particles synthesis.** 10 mL of 1% v/v CD oil-in-water emulsion containing 0.25% w/v SDS was mixed with 20 mL of aqueous solution (containing 0.25% w/v SDS) of 1% w/v polystyrene particles at 40 ^{o}C. After 16 h, 10 mL oil-in-water emulsion (containing 0.25% w/v SDS), composed of 13 mmol St, 7 mmol DVB, 0.24 mmol 2, 2'-Azoisobutyronitrile (AIBN) and 7 mmol hydrophilic anchoring monomer methacrylamide (MAM), was prepared by ultrasonic emulsification and subsequently was added into above solution at 40 ^{o}C for 6 h. After additional adding 5 mL of 1% w/v PVA into the mixture and then deoxygenation bubbled with N_2 for 15 min at room temperature, the polymerization was performed at 70 ^{o}C for 14 h.

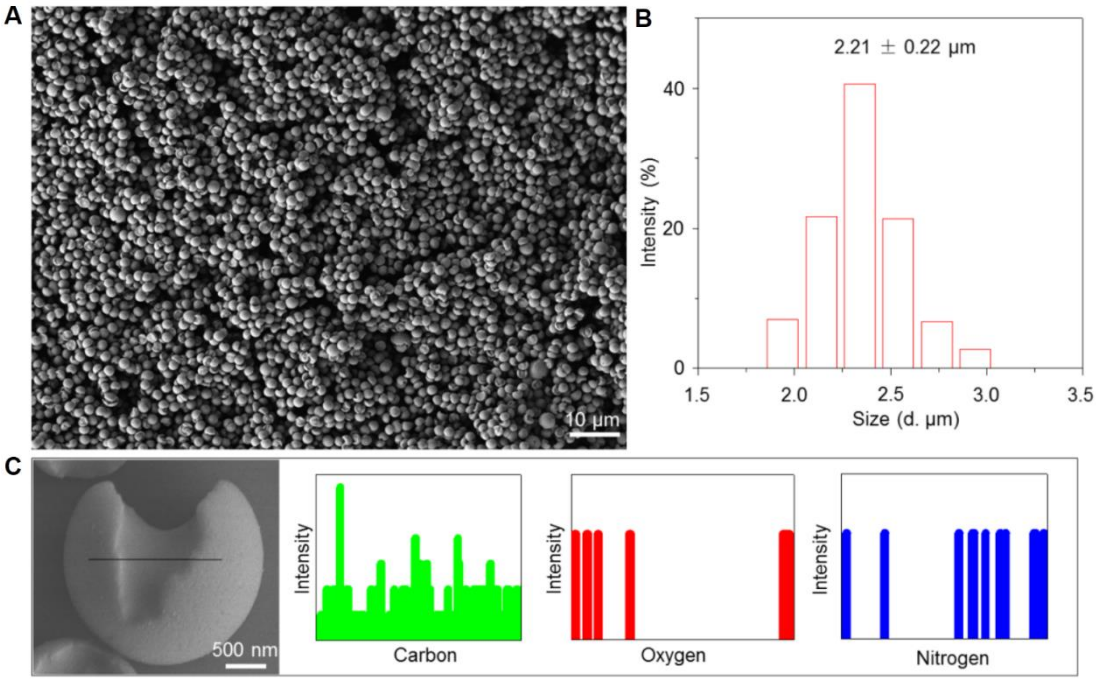

fig. S15. Characterization of crescent moon–shaped PSDVB ⊃ PMAM particles. (**A**) SEM image of large area of particles. (**B**) Particle size distribution analysis of the crescent-moon shaped particles. 300 particles are measured to get the size distribution. (**C**) EDX analysis of Janus particles. The detected elements in polymer particles mainly include C, O and N. The convex region of particles is polymethacrylamide and therefore the detected elements include C, O and N, while the concave region is poly(styrene-co-divinyl benzene) and the detected elements only is C. The results reveal distinct element distributions on the convex surface and concave surface of particles.

5. Characterization of positively charged inorganic nanocrystals

We chose PSDVB ⊃ PAA particles as an example to demonstrate the surface functionalization of Janus particles. Owing to the electronegative properties of convex surface of PAA in PSDVB ⊃ PAA Janus particles, we synthesized charge electropositive Ag and Fe_3O_4 nanoparticles to investigate their interactions.

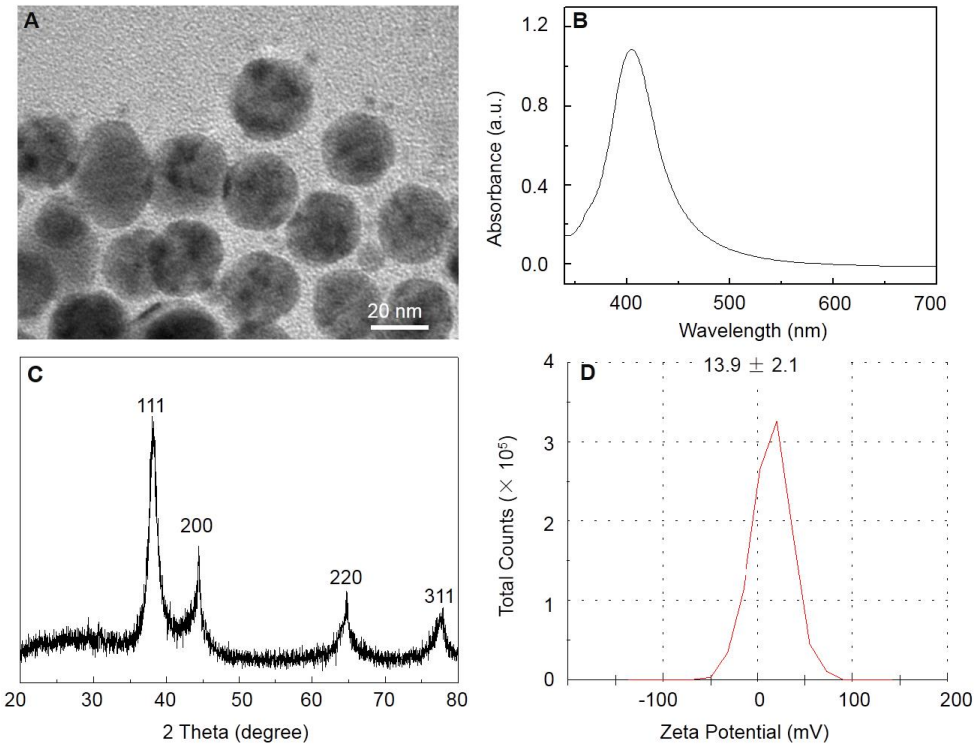

fig. S16. Ag nanoparticle characterization. (**A**) TEM. (**B**) UV-Vis absorbance spectrum. (**C**) XRD spectrum. (**D**) Zeta potential.

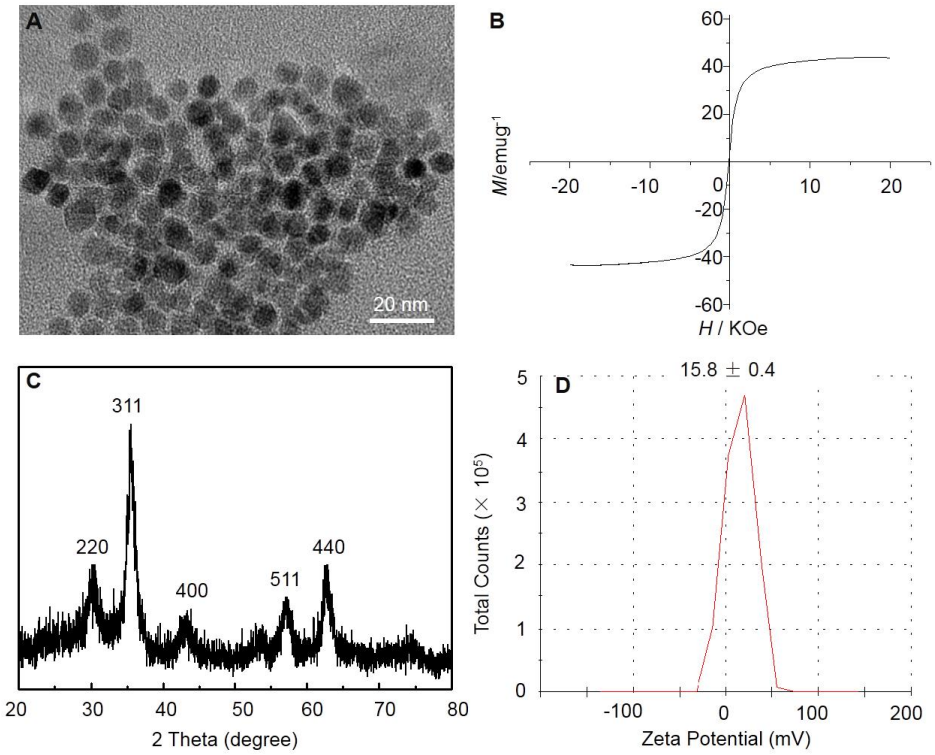

fig. S17. Fe_3O_4 nanoparticle characterization. (**A**)TEM. (**B**) Hysteresis loop of the Fe_3O_4 nanoparticles at room temperature. (**C**) XRD spectrum. (**D**) Zeta potential.

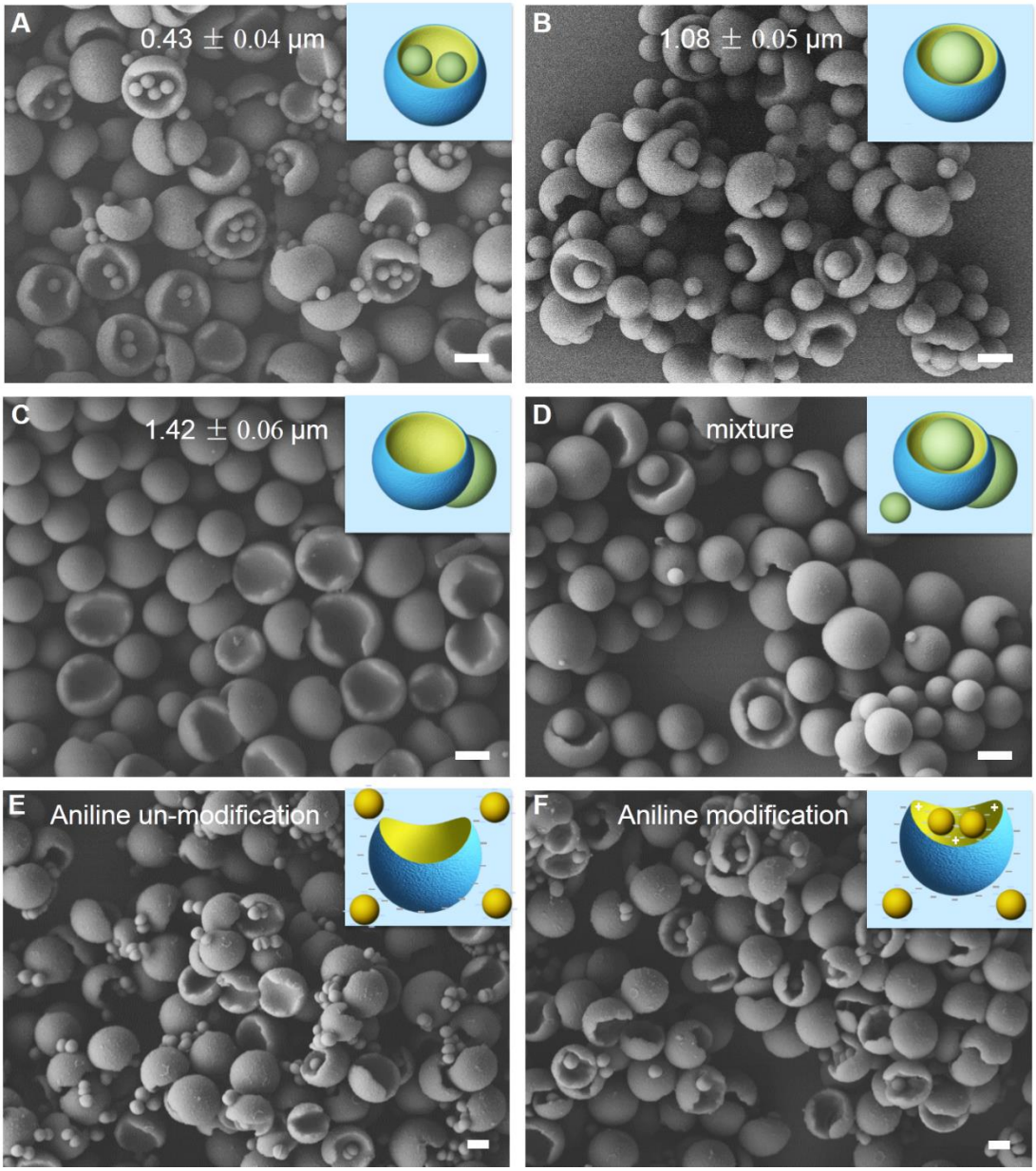

fig. S18. SEM images of the Janus particles capture and recognize spherical PS particles and live bacteria. (**A**) Janus particles capture PS particles with average diameters of 0.43 μm. Scale bar, 1 μm. (**B**) Janus particles capture PS particles with average diameters of 1.08 μm. Scale bar, 1 μm. (**C**) Janus particles capture PS particles with average diameters of 1.42 μm. Scale bar, 1 μm. (**D**) Janus particles capture three different sizes of PS particles (the size of 0.43 μm, 1.08 μm and 1.42 μm). Scale bar, 1 μm. (**E**) Aniline un-modified Janus particles recognize live bacteria. Scale bar, 1 μm. (**F**) Aniline modified Janus particles recognize live bacteria. Scale bar, 1 μm.

The references cited in the Supplementary Materials can be found in the text.